[2] Reshotko, E. and Haefeli, R. C., "Investigation of axially symmetric and two-dimensional multi-nozzles for producing supersonic streams," NACA RM E52H28 (1952).

[3] Gould, L. I., "Preliminary investigation of the supersonic flow field downstream of wire-mesh nozzles in a constant-area duct," NACA RM E51F25 (1951).

[4] Adler, A. A., "Variation with Mach number of static and total pressures through various screens," NACA Wartime Rept. L-23; originally issued as Confidential Bull. L5F28 (February 1946).

[5] Cornell, W. G., "Losses in flow normal to plane screens," Trans. Am. Soc. Mech. Engrs. **80**, 791–799 (1958).

Exhaust Measurements on the Plasma from a Pulsed Coaxial Gun

D. E. T. F. Ashby,* T. J. Gooding,†
B. R. Hayworth,‡ and A. V. Larson§
General Dynamics/Astronautics, San Diego, Calif.

Introduction

Although several groups have investigated pulsed plasma guns for electric propulsion,[1–4] exhaust measurements have been limited mainly to the determination of gross parameters such as total energy content and momentum.[5] More detailed information on the exhaust characteristics is desirable for a better understanding of the acceleration mechanisms. A simple technique of measuring ion current is described with which ion densities up to 3×10^{13} cm^{-3} and ion velocities from 10^6 to 10^7 cm-sec^{-1} have been determined as a function of time and position in the nitrogen plasma from a coaxial gun. The technique has been used previously on high energy hydrogen plasmas produced by guns used in controlled thermonuclear research;[6,7] it is similar to a technique used for examining ion beams.[8]

Description of the Apparatus

The coaxial gun used has been described elsewhere;[3] it produces a burst of nitrogen plasma, containing approximately 10^{18} ions, which travels at several centimeters per microsecond. The probe used to measure ion current is a negatively biased Faraday cup completely surrounded by a grounded shield containing a small entrance hole for the plasma and several pumping holes to ensure that the neutral particle density inside the probe is low. Diagrams of the probe and the biasing circuit are shown in Fig. 1, together with a typical oscillogram of the probe output. The probe is mounted so that it can be moved to different positions in the exhaust.

The cup is biased sufficiently negative so that all the electrons in the plasma which enter the probe are repelled from the cup while the ions are collected. For a plasma of predominately one ion species, the amplitude of the ion current collected (I) is

$$I = nev\,AZ \qquad (1)$$

Presented as Preprint 64-705 at AIAA Fourth Electric Propulsion Conference, Philadelphia, Pa., August 31–September 2, 1964; revision received January 14, 1965. This work was supported by NASA on Contract No. NAS 3-2594.

* Consultant, Space Science Laboratory; on leave of absence from Culham Laboratory, England.

† Senior Staff Scientist, Plasma Propulsion Group, Space Science Laboratory. Member AIAA.

‡ Staff Scientist Plasma Propulsion Group, Space Science Laboratory. Member AIAA.

§ Staff Scientist, Plasma Propulsion Group, Space Science Laboratory.

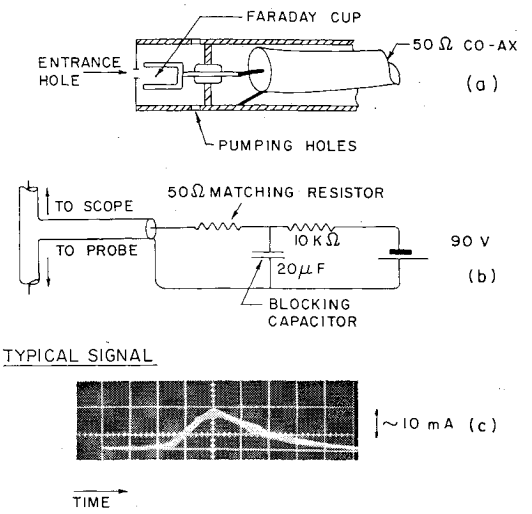

Fig. 1 a) Ion probe; not to scale; over-all diameter 1.5 cm. b) Biasing circuit. c) Typical signal, 8 trace overlay; 5 μsec/cm, flight distance 136 cm, entrance hole 0.5-mm diam.

where n is the ion number density, e is the electronic charge, v is the component of ion velocity normal to the face of the probe, A is the area of the entrance hole, and Z is the number of electronic charges per ion.

If the flight distance is much greater than the gun length and if the transit time greatly exceeds the electrical period, then the plasma can be considered as originating from a point source; therefore, the velocity v of the plasma can be calculated from the time of flight. With v known, nZ is obtained from the amplitude of the ion current. For example, the oscillogram in Fig. 1 shows that the plasma corresponding to the peak in ion current arrives at the probe with a velocity of 6.5 cm/μsec and, if singly ionized, has an ion density of 6.5×10^{12} cm^{-3}.

Experimental Results

The bias voltage necessary to repel electrons from the ion collector is two or three times the electron temperature in electron volts plus any potential difference between the outer

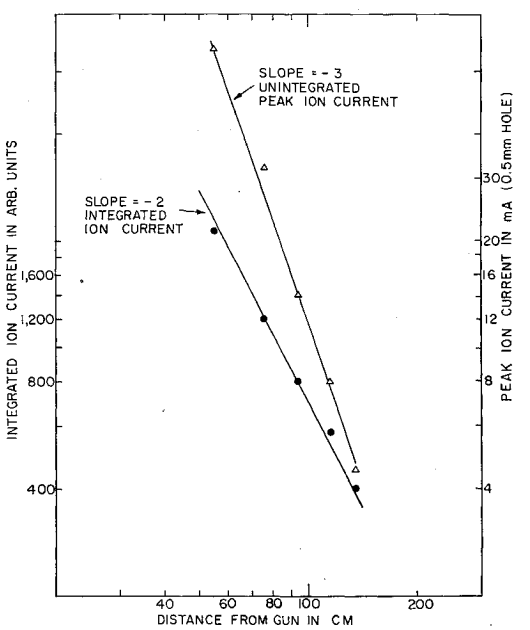

Fig. 2 Probe ion current vs distance from the gun. Gun operating conditions differ from those for Fig. 1c.

shield of the probe and the plasma. The magnitude and polarity of the latter voltage depends on the operating conditions of the gun and, in practice, 50–100 v of bias were necessary.

The distance between the probe and gun was varied from 50 to 150 cm in order to check the behavior of the probe with different plasma densities and to establish whether the gun could be considered as a point source. Figure 2 shows the variation of peak ion current and integrated ion current with distance from the gun. The ion current was integrated with a simple r.c. circuit. The peak current decays inversely as distance cubed, whereas the total number of charges collected varies inversely as distance squared. Therefore, the gun can be treated as a point source of plasma in both space and time. The maximum ion density measured with the probe was 3×10^{13} cm^{-3}

The size of the entrance hole is not critical so long as the ion current does not cause an appreciable drop in the bias voltage; there is no need to keep the entrance hole small compared with the Debye shielding distance. The ion current should be directly proportional to the area of the entrance hole; to verify this, a cluster of ion probes with different size entrance holes was made. Figure 3 shows the variation of peak ion current with hole diameter.

Secondary electrons from the collector will contribute to the total current collected; however, published data indicates that the secondary electron coefficient is small as long as the ion energy is below 1 kev.[9] A small photoelectron current is often recorded as the gun fires; however, it has stopped by the time the probe starts to record ion current. Reflection of plasma from the walls of the vacuum chamber into the entrance or pumping holes can cause errors. In a tank 3 ft $\times$ 3 ft $\times$ 4 ft, the presence of reflected plasma could be detected when the probe was close to a wall.

To check the absolute amplitude of the ion probe signal, the energy-per-unit area in the exhaust was measured with a small calorimeter. The calorimeter had a receiving area of 20.3 cm^2 and was re-entrant so that energy in ablated material would not be lost; it was surrounded by two reflecting shields to reduce radiation losses. The calorimeter measured an average energy density of 0.026 joules/cm^2 per shot. The ion current from a probe at the same position in the exhaust was used to calculate the energy flux due to ion motion. On the assumption that the ions were all singly ionized, the average energy density was calculated to be 0.031 joules/cm^2 per shot. This result is in rough agreement with the calorimeter measurement but ignores the presence of N^{++} in the exhaust.

Since velocity is known through time-of-flight measurements, the abundance of N^{++} and N^{+} could be measured, in principle, by magnetic or electrostatic deflection analyzers; however, with the plasma densities encountered here (10^{11} to 10^{12} cm^{-3}), their use is prohibited by the space charge expansion of the ion beam which occurs within the analyzer. The density attenuation (10^3–10^4) needed was considered excessive

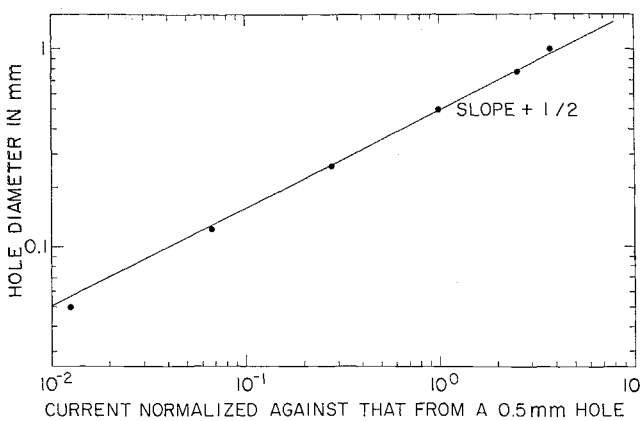

Fig. 3 Probe ion current vs entrance hole size.

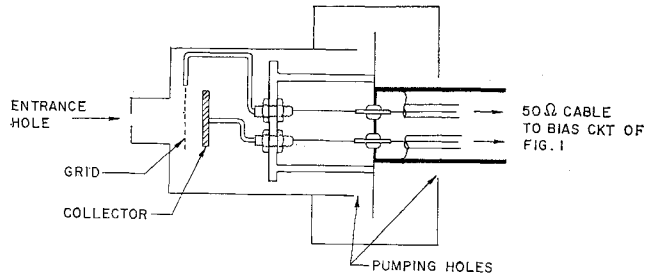

Fig. 4 The gridded analyzer: not to scale; over-all length 10 cm, diameter 10 cm.

for this experiment. Consequently, a simple gridded repeller-type analyzer was used. In contrast to the deflection analyzers, it can work at much higher densities, is much less bulky, but has inherently poorer resolution.

The gridded analyzer is shown in Fig. 4. The negative grid behind the entrance hole repels electrons, whereas the positive collecting plate behind the grid accepts only those ions whose kinetic energy satisfies the following relationship:

$$\tfrac{1}{2}Mv^2 > V_cZe \qquad (2)$$

where V_c is the positive potential of the collecting plate. The signal from the first grid varies as the total ion current entering the probe, whereas the collector current is proportional to the current from the fraction of ions which satisfy Eq. (2).

Two points about the use of the gridded analyzer should be noted. Firstly, any potential difference between the plasma and the probe will produce a plasma sheath, which alters the energies of the incoming ions; this effect, which is common to all analyzers, can be appreciable for low energy particles. Secondly, the mesh size of the grid must be much less than the Debye shielding distance appropriate to the grid voltage and the plasma density.

The oscillograms in Fig. 5 illustrate the performance of the analyzer. In each picture the upper trace is the current to the negative grid, and the lower trace is the current to the positive collector. The current to the collector reduces progressively as its potential is increased. Two marked cutoffs occur which correspond to N^{++} and N^{+} ions, the N^{++} cutoff occurring earlier in time. The oscillograms show that approximately 70% of the plasma is doubly ionized.

When a correction is made for the percentage of N^{++} in the exhaust, the ion probe shows that the energy density due to

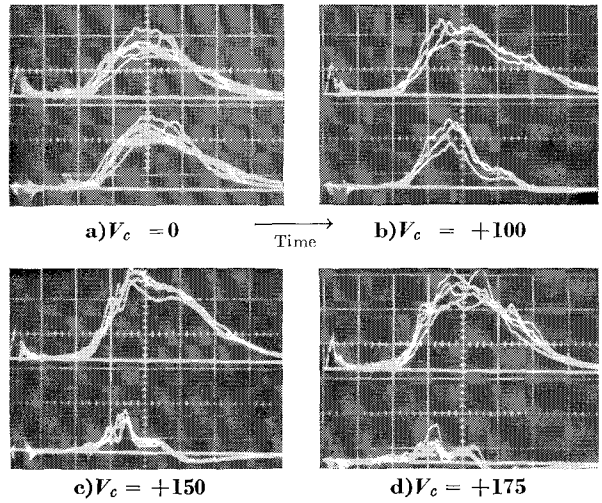

Fig. 5 Gridded analyzer oscillograms: upper trace in each is grid current, grid biased to -100 v; lower trace is collector current, collector biased to $+V_c$ v; 5 μsec/cm, flight distance 112 cm.

kinetic motion of the ions is 0.0185 joules/cm² per shot; an additional 0.0015 joules/cm² per shot is present in ionization energy. The combined energy density is 0.020 joules/cm² per shot compared with the total energy density of 0.026 joules/cm² per shot given by the calorimeter. Although the two results are within experimental error, the higher figure given by the calorimeter could be attributed to fast neutrals.

Conclusions

The agreement between the energy density inferred from the ion probe results and the energy density measured with a calorimeter shows that the ion probe can give quantitative information in a tenuous nitrogen plasma having a directed energy of a few hundred electron volts. The simplicity and compact size of the ion probe, with or without an analyzing grid, makes it ideal for probing the exhaust plasmas from pulsed plasma guns.

References

[1] Stuhlinger, E., "Electric propulsion—1964," Astronaut. Aeronaut. **2**, 26 (1964).

[2] Longmire, C. L., "The use of plasma for propulsion of interplanetary rockets," pp. 3–11; Starr, W. L. and Naff, J. T., "Acceleration of metal-derived plasmas," pp. 47–59; Marshall, J., "Hydromagnetic plasma gun," pp. 60–72; Gartenhaus, S. and Tannenwald, L. M., "Propulsion from pinch collapse," pp. 73–78, *Plasma Acceleration*, edited by S. W. Kash (Stanford Univ. Press, Stanford, Calif., 1960).

[3] Larson, A. V., Gooding, T. J., Hayworth, B. R., and Ashby, D. E. T. F., "An energy inventory in a coaxial plasma accelerator driven by a pulse line energy source," AIAA J. **3**, 977–979 (1965).

[4] Duclos, D. P., Aronowitz, L., Fessenden, F. P., and Carstensen, P. B., "Diagnostic studies of a pinch plasma accelerator," AIAA J. **1**, 2505–2513 (1963).

[5] Gooding, T. J., Hayworth, B. R., and Lovberg, R. H., "Use of ballistic pendulums with pulsed plasma accelerators," ARS J. **32**, 1599 (1962).

[6] Coensgen, F. H., Sherman, A. E., Nexsen, W. E., and Cummins, W. P., "Plasma injection into a magnetic field of cusped geometry," Phys. Fluids **3**, 764 (1960).

[7] Ashby, D. E. T. F., "The flow of high energy plasma in a magnetic guide field," Proc. Intern. Conf. Ionization Phenomena Gases, 6th, Paris **4**, 465–468 (1963).

[8] Moore, D. and Kinzie, P., "Diagnostics of the space charge neutralization of ion beams by electron injection," *AIAA Progress in Astronautics and Rocketry: Electrostatic Propulsion*, edited by David B. Langmuir, Ernst Stuhlinger, and J. M. Sellen, Jr. (Academic Press Inc., New York, 1961), Vol. 5, pp. 457–471.

[9] McDaniel, E. W., *Collision Phenomena in Ionized Gases* (John Wiley and Sons, Inc., New York, 1964), pp. 629–658.

Dynamic Response of an Encased Elastic Cylinder with Ablating Inner Surface

J. D. Achenbach*
Northwestern University, Evanston, Ill.

Introduction

THE loss of mass and stiffness affects the dynamic response of a structure. Previous work in this area[1] is related to re-entry problems, where the stiffness of the thin covering layer of ablative material is neglected, and only the influence of the mass loss is taken into account. In studying the dynamic response of a burning cylindrical-grain in a solid-propellant rocket, the influence of the stiffness of the solid-propellant material cannot be ignored. The present note is a study of the forced vibrations of an encased elastic cylinder with an ablating inner surface.

A time-dependent internal pressure is applied at the inner surface of the cylinder. If the cylinder were of a compressible elastic material the problem would concern cylindrical waves that emanate from the moving inner surface and interact with the surrounding shell. Since the ablation rate is very small as compared to the dilatational wave velocity, a vibrationary type of response would set in after a short time. In this note the cylinder material is assumed to be incompressible. As a consequence, the wave velocity of dilatational waves is infinite, and a forced vibration is immediately started without initial wave effects. It may be mentioned that solid-propellant materials show very high bulk moduli and are usually considered incompressible.

Special attention has been devoted to the circumferential stress at the ablating inner surface. The analysis is valid for arbitrary ablation rates.

Statement of the Problem

A long elastic cylinder is considered with a circular port of monotonically increasing radius $a(t)$ and a constant outer radius b at which the cylinder is bonded to a thin elastic shell. Both the cylinder and the surrounding shell are maintained in a state of plane strain.

If the cylinder is under the action of an internal pressure the equation of motion is expressed as

$$\partial\sigma_r/\partial r + (\sigma_r - \sigma_\theta)/r = \rho_p(\partial^2 u/\partial t^2) \tag{1}$$

In Eq. (1) r and θ are the polar coordinates, and u is the displacement in the radial direction. The subscript p denotes a material constant of the cylinder.

For an incompressible elastic cylinder the radial displacement is of the form

$$u = k(t)/r \tag{2}$$

where $k(t)$ is a function of t only.

Let s_{ij} and e_{ij}, respectively, denote the components of deviatoric stress and strain. The stress-strain relation for the incompressible elastic material can then be expressed in the form

$$s_{ij} = 2\mu e_{ij} \tag{3}$$

From Eq. (3) we derive

$$\sigma_r - \sigma_\theta = 2\mu(\epsilon_r - \epsilon_\theta) = -4\mu k(t)/r^2 \tag{4}$$

The radial stress is prescribed at $r = a(t)$ as

$$r = a(t): \quad \sigma_r = -\sigma_i(t) \tag{5}$$

The radial stress at $r = b$ is derived from the equation of motion of an element of the thin surrounding shell. With the requirements that the radial stress and the circumferential strain are continuous at the cylinder shell interface, we obtain

$$[\sigma_r]_{r=b} = -(h/b)\,(E'/b^2)\,k(t) - \rho_s\,(h/b)\,\ddot{k}(t) \tag{6}$$

In Eq. (6), $E' = E_s/(1 - \nu_s^2)$, and ν_s is Poisson's ratio. A subscript s denotes a material constant of the shell (case). The thickness of the case is denoted by h.

The expressions for u and $\sigma_r - \sigma_\theta$, respectively Eqs. (2) and (4), are now substituted into Eq. (1), and the resulting equation for σ_r is subsequently integrated with respect to r. Taking into account that the radial stress is prescribed at the ablating inner surface Eq. (5) and at $r = b$ Eq. (6), we obtain the following differential equation for $k(t)$:

$$\left\{\rho_p \ln\left[\frac{b}{a(t)}\right] + \rho_s\left(\frac{h}{b}\right)\right\}\ddot{k}(t) - \left\{2\mu\left[\frac{1}{b^2} - \frac{1}{a(t)^2}\right] - \left(\frac{h}{b}\right)\frac{E'}{b^2}\right\}k(t) = \sigma_i(t) \tag{7}$$

Received October 26, 1964. This work was supported by the Office of Naval Research under Contract ONR Nonr. 1228(34) with Northwestern University.

* Assistant Professor, Department of Civil Engineering. Member AIAA.